

Published in final edited form as:

*Stroke*. 2012 November ; 43(11): 2962–2967. doi:10.1161/STROKEAHA.112.656058.

## Multivoxel MR Spectroscopy in Acute Ischemic Stroke: Comparison to the Stroke Protocol MRI

Krishna A. Dani, MRCP, PhD, Li An, PhD, Erica C. Henning, PhD, Jun Shen, PhD, and Steven Warach, MD, PhD on behalf of the National Institute of Neurological Disorders and Stroke Natural History of Stroke Investigators

Section on Stroke Diagnostics and Therapeutics, National Institute of Neurological Disorders and Stroke, Bethesda, MD (K.A.D., L.A., E.C.H., S.W.); and the National Institute of Mental Health, National Institutes of Health, Bethesda, MD (J.S.)

### Abstract

**Background and Purpose**—Few patients with stroke have been imaged with MR spectroscopy (MRS) within the first few hours after onset. We compared data from current MRI protocols to MRS in subjects with ischemic stroke.

**Methods**—MRS was incorporated into the standard clinical MRI stroke protocol for subjects <24 hours after onset. MRI and clinical correlates for the metabolic data from MRS were sought.

**Results**—One hundred thirty-six MRS voxels from 32 subjects were analyzed. Lactate preceded the appearance of the lesion on diffusion-weighted imaging in some voxels but in others lagged behind it. Current protocols may predict up to 41% of the variance of MRS metabolites. Serum glucose concentration and time to maximum partially predicted the concentration of all major metabolites.

**Conclusion**—MRS may be helpful in acute stroke, especially for lactate detection when perfusion-weighted imaging is unavailable. Current MRI protocols do provide surrogate markers for some indices of metabolic activity.

### Keywords

magnetic resonance spectroscopy; spectroscopy; stroke

---

Although MRI offers truly multimodal imaging of acute ischemic stroke, recent focus has been on the perfusion–diffusion mismatch hypothesis.<sup>1</sup> Although this concept has not been fully validated, modifications to its application in ongoing studies may hold the key to identifying potentially salvageable tissue—the ischemic penumbra. Nonetheless, other MRI modalities may have a role in refining therapeutic decisions. MR spectroscopy (MRS) has previously been suggested to be of value and could potentially identify the ischemic penumbra. For example, preservation of N-acetyl-L-aspartate (NAA; neuronal integrity) with increased lactate (anaerobic glycolysis) is an attractive potential marker of the ischemic penumbra.<sup>2</sup> Although the changes in the “major” spectroscopic metabolites have been well documented in the subacute phase of stroke and beyond,<sup>3–7</sup> there has been only limited evaluation of the behavior of these metabolites in the acute phase,<sup>8–10</sup> especially within the

---

Copyright © 2012 American Heart Association, Inc. All rights reserved

Correspondence to Steven Warach, MD, PhD, Professor and Executive Director, Seton/UT Southwestern Clinical Research Institute of Austin Vice-Chair for Austin Programs, Department of Neurology and Neurotherapeutics UT Southwestern Medical Center, 1400 N IH 35, Suite 2.240, Austin, TX 78701. swarach@seton.org; steven.warach@utsouthwestern.edu.

**Disclosures** None.

thrombolysis time window. In addition, it is unclear how these metabolite changes correspond to modern MRI stroke protocols and whether MRS can offer any additional useful information.

In this multivoxel MRS study, we evaluated metabolite changes within conventionally defined tissue compartments and investigated whether MRS can provide additional useful information.

## Methods

### Subjects

This was a retrospective analysis of a prospectively acquired data set from Washington Hospital Center, Washington, DC, performed in compliance with local Institutional Review Board requirements. MRS data were acquired as part of the routine MR stroke protocol between October 2008 and January 2010 at the discretion of the treating clinicians. After identification of subjects with MRS data, the inclusion criteria into this current study were that the patients had (1) imaging evidence of hemispheric ischemic stroke; and that (2) MRS data were acquired at  $\leq 24$  hours; and were (3) evaluable; and (4) voxels were overlying a diffusion-weighted imaging (DWI) or perfusion-weighted imaging (PWI) lesion. There was no threshold for severity for inclusion into the study. Data were excluded if (1) subjects declined permission for data to be used for research; or (2) if there was a previous stroke in the region of the lesional or ipsilesional voxels.

### Data Acquisition

We incorporated a single-slice multivoxel spectroscopy sequence into our routine acute stroke MRI protocol. All scans were acquired using a 3.0-T Philips Achieva whole-body scanner (Philips Medical Systems, Best, The Netherlands). The MRS sequence was performed after acquisition of all other sequences in the series and was localized to the isotropic image from DWI. The MRS volume of interest (VOI) covered 12 mm in the z direction and therefore incorporated DWI slices. The VOI was therefore centered on the image slice that was of most interest, as guided by the DWI and PWI data. This was achieved by prescribing the coordinates and the angulation of the desired central DWI slice for the chemical shift imaging VOI. In the chemical shift imaging preparation scan, first-order shimming and chemical shift selective water suppression were optimized for the VOI. The chemical shift imaging data were acquired using Point Resolved Spectroscopy excitation. Parameters of this sequence are as follows: TR=2 seconds, TE=144 ms, matrix=12 $\times$ 12, field of view=12 $\times$ 12 cm<sup>2</sup>, VOI=10 $\times$ 10 $\times$ 1.2 cm<sup>3</sup>, signal averages=1, duration=5 minutes. The parameters of the PWI, DWI, and fluid-attenuated inversion recovery (FLAIR) imaging varied according to continuing modification of these sequences.

### Postprocessing

**MRS Data**—Imaging data were loaded into in-house software written in Interactive Data Language (IDL Version 7.0; Research Systems Inc, Boulder, CO), and the MRS matrix grid was overlaid on a user-selected MR image (typically toggled between DWI and PWI). Ipsilesional voxels were selected if  $>50\%$  of the voxel covered either DWI lesion or PWI deficit (on any of the unthresholded maps) by visual inspection. We did not derive data from the outermost voxels (ie, the 42 voxels most peripheral on the matrix of voxels) to avoid artifact. In addition, 4 to 8 contralateral voxels were also analyzed as a reference. This allowed us to cover the “mirror” region without incorporating signal from tissue interfaces. Selecting more voxels than this number meant the selection of voxels distant to the “mirror” region. These contralateral voxels were selected in a region that matched the region underlying the ipsilesional voxels as closely as possible. An automatic peak-fitting

procedure was performed on each voxel using a Levenberg-Marquardt optimization subroutine. Peak area (metabolite concentration), line width, and signal-to-noise ratio were computed for each metabolic peak after peak fitting. If there was evidence of lipid or water contamination, the voxel was termed “unevaluable.” MRS results were graphed on a standard abscissa with metabolite concentrations recorded for NAA (2.01 ppm), lactate (Lac; 1.33 ppm), choline (Cho; 3.22 ppm), and total creatine (tCr; 3.03 ppm).

**MRI Stroke Protocol Data**—PWI postprocessing was performed with Stroketool (Version 2.4; Digital Imaging Solutions), which uses standard singular value decomposition. An arterial input function was defined by selecting 5 voxels from the M1 segment of the contralesional middle cerebral artery. Motion correction and a 3×3 Gaussian spatial smoothing algorithm were implemented. Maps of time to maximum of the residue function (TMAX) were produced thereafter. Maps of regional cerebral blood volume (rCBV) were also produced. We did not use a deconvolution routine for rCBV because we found that the non-deconvolved approach produced less signal dropout in profoundly hypoperfused tissue.

Maps of b0 and b1000 from DWI were loaded into in-house software written in IDL to create maps of apparent diffusion coefficient (ADC). To filter out voxels containing cerebrospinal fluid, an upper threshold of 1.3 mm<sup>2</sup>/s was set.

**Derivation of Values From Individual Voxels**—Medical Imaging, Processing and Visualization Software (MIPAV, Version 4.3; National Institutes of Health, Bethesda, MD) was used. FLAIR, TMAX, and rCBV maps were coregistered to DWI using trilinear coregistration. The MRS matrix was exported from the MRS software and converted to a VOI in MIPAV. This VOI was then overlaid on each individual MR image or map, and individual voxels from within the VOI were assessed. Voxels were graded for PWI and DWI over 3 slices as 1=all voxel covering lesion, 2=most of voxel covering lesion (ie, >50%), 3=some voxel covering lesion (ie, <50%), 4=no voxel filled with lesion, 5=data uninterpretable. A voxel was classified as DWI lesion or PWI deficit if it fulfilled criteria 1 or 2 on DWI or PWI, respectively, as hypoperfused DWI lesion if it fulfilled criteria 1 or 2 on both DWI and PWI, and as PWI–DWI mismatch if it fulfilled criteria 3 or 4 for DWI lesion and 1 or 2 for PWI deficit.

Quantitative data were extracted for each ipsilesional voxel, which was included. MIPAV allowed averaged values for TMAX and ADC to be extracted. We calculated rrCBV as the rCBV value in the voxel divided by the rCBV in the reference region. For FLAIR data, a qualitative ordinal scale was applied: 1=normal intensity, 2=subtle hyper-intensity, and 3=bright. An averaged value for each parameter was recorded for the contralesional voxels.

**Derivation of Values From Individual Subjects**—For any given tissue compartment, metabolic data from individual voxels were averaged to produce a single value for metabolic concentration.

## Statistical Analysis

The software StatsDirect ([www.statsdirect.com](http://www.statsdirect.com)) was used. Statistical significance was defined as  $P < 0.05$ . MRS data were expressed as the concentration of metabolite in the ipsilesional voxel divided by the sum of contralesional NAA, tCr, and Cho, for example, [metabolite/sum]. Nonparametric tests were used when data were found to be nonnormal (Shapiro-Wilk test). When averaged metabolite data for individual subjects were compared with other clinical parameters (glucose, DWI lesion volume, time since onset), the Spearman correlation was used. The Mann-Whitney test was used to compare metabolite data from individual voxels between PWI–DWI mismatch versus DWI lesion and hypoperfused versus

perfused DWI lesion. Multiple linear regression analysis determined the degree to which MR parameters predicted the concentration of individual metabolites. TMAX, rrCBV, ADC, and FLAIR hyperintensity (2 dummy variables: subtle and bright) were entered as predictors of each individual metabolite ([metabolite/sum]). After entering only these radiological variables into the model, we then added 2 clinical variables (serum glucose and time since onset). Negative correlations are denoted by the prefix “-.”

## Results

### Subjects

Data from 32 subjects (18 male) yielded 136 voxels. Six scans were acquired immediately after recombinant tissue-type plasminogen activator because there was no baseline MRS available; the remainder was acquired at baseline. Mean age was 66 years (SD=13.2), median National Institutes of Health Stroke Scale was 10 (interquartile range, 5–18), and median time to imaging was 4.5 hours (range, 1.28–24 hours; interquartile range, 2.7–7.8 hours). Lesion volume on DWI was 18 mL (range, 0–291 mL; interquartile range, 5–80 mL). DWI lesion volume showed a significant positive correlation with admission National Institutes of Health Stroke Scale ( $\rho=0.77$ ,  $P<0.0001$ ). Basic clinic–radiological data are presented in the Table.

### Spectroscopy Data From Individual Subjects

The median number of ipsilesional voxels from each subject was 3 (range, 1–12; interquartile range, 2–7). For subject-wise data, lactate (Lac/sum) showed a significant positive correlation with admission glucose ( $\rho=0.42$ ,  $P=0.018$ ; Figure 1). This relationship was not seen with any other metabolite: NAA/sum ( $P=0.2$ ), Cho/sum ( $P=0.25$ ), tCr/sum ( $P=0.5$ ). There was no significant correlation between metabolite concentration and DWI lesion volume (Lac/sum,  $P=0.09$ ; NAA/sum,  $P=0.07$ ; Cho/sum,  $P=0.52$ ; Cr/sum,  $P=0.58$ ) or time since onset (Lac/sum,  $P=0.51$ ; NAA/sum,  $P=0.89$ ; Cho/sum,  $P=0.09$ ; Cr/sum,  $P=0.82$ ). The statistical significance of these findings was no different if only voxels that were predominantly or exclusively filled by DWI lesion were analyzed ( $n=29$  subjects,  $n=111$  voxels).

### Spectroscopy Data From Individual Voxels

Of the 136 voxels, 5 voxels were unevaluable. For Subject 27, there were no contralateral voxels available for analysis owing to suboptimal placement of the voxel matrix, and therefore ipsilesional voxels ( $n=3$ ) from this subject were not analyzed. The remaining 128 voxels were analyzed fully. Of these voxels, 111 were completely ( $n=26$ ) or mostly ( $n=85$ ) covering DWI lesion and of these, 66 (60%) were completely ( $n=26$ ) or mostly ( $n=40$ ) hypoperfused. Six voxels covered hypoperfused regions with no DWI lesion, and 11 voxels covered hypoperfused voxels, which were partially (<50%) affected by DWI lesion, in a “reverse mismatch” pattern.

Metabolite data were transformed using a natural logarithmic function to produce satisfactorily distributed residuals. For transformed Lac/sum, TMAX ( $P=0.005$ ,  $r=0.27$ ), ADC ( $P=0.004$ ,  $r=-0.27$ ), and FLAIR (subtle hyperintensity  $P=0.0016$ ,  $r=-0.3$ ) but not rrCBV ( $P=0.2$ ) were independent predictors ( $R^2=0.25$ ). When the clinical variables were included ( $R^2=41\%$ ), ADC became an insignificant predictor ( $P=0.15$ ) along with rrCBV ( $P=0.84$ ) and time since onset ( $P=0.22$ ). Admission glucose ( $P<0.0001$ ,  $r=0.47$ ), FLAIR hyperintensity ( $P=0.049$ ,  $r=-0.2$ ), and TMAX ( $P=0.016$ ,  $r=0.23$ ) were significant predictors. For transformed NAA/sum, all radiological parameters were independent predictors ( $R^2=0.26$ ) with ADC showing the strongest correlation: TMAX ( $P=0.004$ ,  $r=0.26$ ); ADC ( $P<0.0001$ ,  $r=0.43$ ); rrCBV ( $P=0.02$ ,  $r=-0.2$ ); and FLAIR (subtle hyperintensity,  $P=0.049$ ,

$r=-0.2$ ). When clinical variables were added to the model ( $R^2=30\%$ ), TMAX ( $P=0.01$ ), ADC ( $P<0.0001$ ), rrCBV ( $P=0.006$ ), and admission glucose ( $P=0.02$ ,  $r=0.2$ ) were predictors, with FLAIR losing significance ( $P=0.16$ ) and time since onset being insignificant ( $P=0.9$ ). For transformed Cho/sum, only FLAIR predicted the relative concentration (subtle hyperintensity,  $P=0.015$ ,  $r=-0.22$ ,  $R^2=9.2\%$ ) when only radiological parameters were considered. The remaining variables were insignificant predictors: TMAX ( $P=0.18$ ), ADC ( $P=0.22$ ), and rrCBV ( $P=0.32$ ). When clinical variables were added to the model, admission serum glucose ( $P=0.0041$ ,  $r=0.27$ ) and ADC value ( $P=0.03$ ,  $r=0.2$ ) were significant predictors ( $R^2=16\%$ ) with FLAIR losing significance ( $P=0.09$ ) and no other predictor being significant ( $P=0.2$ ). For transformed tCr/sum, only TMAX ( $P=0.001$ ,  $r=0.3$ ) was a predictor when only radiological variables were considered ( $R^2=0.10$ ): FLAIR ( $P=0.33$ ), ADC ( $P=0.2$ ), and rrCBV ( $P=0.7$ ). Addition of clinical variables (serum glucose,  $P=0.09$ ; time since onset,  $P=0.08$ ) did not substantially improve the predictive value of the model ( $R^2=14\%$ ).

### Analysis of Patterns of Metabolite Distribution

There were 17 voxels from 8 subjects with PWI–DWI mismatch. In 6 of 17 voxels, Lac was detectable in significant concentrations (signal-to-noise ratio  $>2.33$ ). NAA/sum was greater in these voxels ( $n=17$ ) compared with voxels covering DWI lesion ( $n=111$ ; median, 0.49 versus 0.38;  $P=0.0039$ ). The Lac peaks in the mismatch regions were small (median Lac/sum=0.04) in comparison to DWI lesion (median Lac/sum=0.15;  $P<0.0001$ ). There was no difference in Cr ( $P=0.26$ ) or Cho ( $P=0.23$ ) between mismatch and nonmismatch voxels. Of the 17 mismatch voxels, 6 voxels from 3 subjects had no DWI lesion with 3 of these voxels showing Lac. One subject who presented with a right homonymous hemianopia had no DWI lesion at the time of imaging at 1.7 hours (Subject 24), but the deficit on PWI was associated with significant Lac in the left occipital lobe. This region proceeded to infarction at follow-up imaging (Figure 2).

Although Lac was present in most voxels overlying DWI lesions, a small number of voxels did not show Lac at the time of imaging (28 of 111), even when hypoperfused ( $n=21$  of 66). Figure 3 gives an example of a subject with no Lac within the DWI lesion on baseline imaging at 2.2 hours but where Lac was present on follow-up imaging. Finally, there was no significant difference in any metabolite concentration between voxels in hypoperfused DWI lesion ( $n=66$ ) versus voxels where there was some evidence of reperfusion ( $n=32$ ,  $P=0.6$ ).

### Discussion

This is the first human study to demonstrate the use of MRS-defined lactate to identify “tissue at risk” (Figure 2). A small number of voxels overlying the PWI–DWI mismatch region showed preserved NAA concentration but elevated Lac concentration. However, Lac was not always detectable in the early hours after stroke and could still be seen in the reperfused DWI lesion. Radiological parameters all predicted at least some of the variance of metabolite concentration, but in general, FLAIR hyperintensity was a weak predictor. Serum glucose concentration and TMAX predicted the concentration of all 4 metabolites, but “time since onset” was not a significant predictor of metabolite concentration.

How do these results compare with previous investigation? An increase in tissue Lac production is seen with anaerobic metabolism and is detectable at a cerebral blood flow threshold just above that for tissue at risk of infarction.<sup>11</sup> Animal studies have suggested that Lac is detectable within minutes of stroke and that NAA may decrease by as much as 20% in the first hour and 50% in the first 6 hours.<sup>12,13</sup> However, only a handful of studies have focused on patients in the early hours of stroke. Singhal et al<sup>9</sup> demonstrated significant correlations between Lac and NAA with ADC and Nicoli et al<sup>10</sup> described a wide range of



Lac concentrations within a narrow range of ADC values. Munoz Maniega et al<sup>8</sup> demonstrated higher NAA concentrations in the “possibly abnormal” voxels compared with the definitely abnormal voxels, whereas Lac was high in both in 51 subjects <24 hours (50% <6 hours). This current study adds to these previous studies by providing a comprehensive description of metabolite changes in the context of all routinely used MR stroke protocol parameters.

Can MRS sequences be of additional use to the standard MR stroke protocol? Current MRI parameters predicted up to a 41% of the variance seen in the MRS metabolites. It is unclear whether the remaining variance was simply due to noise or whether MRS can add additional metabolic information, but because regions of penumbra can exist within regions of low<sup>14</sup> as well as normal ADC, there is biological rationale to support the latter. Indeed, MRS may also help to refine penumbral definition by PWI–DWI mismatch. It has previously been hypothesized that preserved NAA but detectable Lac may represent the MRS penumbral signature.<sup>2</sup> Our data are supportive of this concept with variable presence of Lac in the mismatch region and demonstration of the presence of Lac preceding infarction. Although we showed that Lac is not specific or entirely sensitive for the PWI–DWI mismatch region, the regions of mismatch that truly represent the ischemic penumbra could potentially be refined by additional consideration of Lac. To test this, a large number of subjects with mismatch at baseline and structural imaging at follow-up would be required. Next, this study also reveals the wealth of information already provided by current MRI protocols. For example, TMAX was a good general marker of metabolic activity, being predictive of neuronal integrity (NAA), energy metabolism (Cr), and anaerobic glycolysis (Lac) and membrane stability (Cho). Finally, this study supports previous findings<sup>15</sup> of a correlation between serum glucose and lactate concentrations. In addition, results from this study suggest that the combination of radiological parameters, especially TMAX, with serum glucose concentration is even more powerful for the prediction tissue viability. Not only does this support previous findings that hyperglycemia<sup>16</sup> and the depth of hypoperfusion<sup>11</sup> influence outcome, but it also suggests that these are independent of each other in their influence. MRS may therefore be a reliable tool for the investigation of the pathophysiology of stroke and that it could potentially define imaging end points in clinical trials.

A number of limitations was associated with this study. Firstly, this was retrospective analysis of a prospectively acquired data set and ongoing adjustments to our stroke MRI protocol may have affected results. Next, this single-slice MRS study may have missed peripheral penumbral regions, which may have had a different metabolic signature. Next, we used the contralesional hemisphere as a reference because the concentration of all major metabolites changes after stroke,<sup>3</sup> making intravoxel metabolite ratios difficult to interpret. Although our approach circumvents these issues, it is susceptible to potential errors introduced by magnetic field inhomogeneities. Next, a longer MRS acquisition time could have increased sensitivity to Lac but would have been less clinically applicable. Other potential explanations for the lack of lactate detection within the DWI lesion include inadequate water suppression, small voxel size, and limited spectral quality due to head movements. Next, the use of multiple linear regression analysis assumed a linear and monotonous relationship between variables. Results should be confirmed in a larger data set, especially when predictors were of borderline significance. In addition, determination of the “penumbral” signature was limited by the small number of voxels, even in this cohort, which was scanned early. Finally, head movement and contamination with scalp lipid may make scans uninterpretable. However, its use beyond the hyperacute window, for example as an end point in a clinical trial, remains a feasible use for this tool.

In conclusion, MRS may provide additional metabolic information but may be difficult to introduce as part of the routine stroke MR protocol. In particular, it may be of use when PWI is unavailable and may be of use to measure end points for clinical trials.

## Acknowledgments

Marie Luby and Karrie Hester provided support with data management.

**Sources of Funding** This research was supported by the Division of Intramural Research of the National Institutes of Health, National Institute of Neurological Disorders and Stroke. Dr Dani was supported by the Patrick Berthoud Charitable Trust.

## References

- Schlaug G, Benfield A, Baird AE, Siewert B, Lovblad KO, Parker RA, et al. The ischemic penumbra: operationally defined by diffusion and perfusion MRI. *Neurology*. 1999; 53:1528. [PubMed: 10534263]
- Gillard JH, Barker PB, van Zijl PC, Bryan RN, Oppenheimer SM. Proton MR spectroscopy in acute middle cerebral artery stroke. *AJNR Am J Neuroradiol*. 1996; 17:873–886. [PubMed: 8733962]
- Saunders DE. MR spectroscopy in stroke. *Br Med Bull*. 2000; 56:334–345. [PubMed: 11092084]
- Duijn JH, Matson GB, Maudsley AA, Hugg JW, Weiner MW. Human brain infarction: proton MR spectroscopy. *Radiology*. 1992; 183:711–718. [PubMed: 1584925]
- Gideon P, Henriksen O, Sperling B, Christiansen P, Olsen TS, Jorgensen HS, et al. Early time course of N-acetylaspartate, creatine and phosphocreatine, and compounds containing choline in the brain after acute stroke. A proton magnetic resonance spectroscopy study. *Stroke*. 1992; 23:1566–1572. [PubMed: 1440704]
- Graham GD, Blamire AM, Rothman DL, Brass LM, Fayad PB, Petroff OA, et al. Early temporal variation of cerebral metabolites after human stroke. A proton magnetic resonance spectroscopy study. *Stroke*. 1993; 24:1891–1896. [PubMed: 8248973]
- Wardlaw JM, Marshall I, Wild J, Dennis MS, Cannon J, Lewis SC. Studies of acute ischemic stroke with proton magnetic resonance spectroscopy: relation between time from onset, neurological deficit, metabolite abnormalities in the infarct, blood flow, and clinical outcome. *Stroke*. 1998; 29:1618–1624. [PubMed: 9707203]
- Munoz Maniega S, Cvorov V, Chappell FM, Armitage PA, Marshall I, Bastin ME, et al. Changes in NAA and lactate following ischemic stroke: a serial MR spectroscopic imaging study. *Neurology*. 2008; 71:1993–1999. [PubMed: 19064881]
- Singhal AB, Ratai E, Benner T, Vangel M, Lee V, Koroshetz WJ, et al. Magnetic resonance spectroscopy study of oxygen therapy in ischemic stroke. *Stroke*. 2007; 38:2851. [PubMed: 17761914]
- Nicoli F, Lefur Y, Denis B, Ranjeva JP, Confort-Gouny S, Cozzzone PJ. Metabolic counterpart of decreased apparent diffusion coefficient during hyperacute ischemic stroke: a brain proton magnetic resonance spectroscopic imaging study. *Stroke*. 2003; 34:e82–e87. [PubMed: 12817104]
- Hossmann KA. Viability thresholds and the penumbra of focal ischemia. *Ann Neurol*. 1994; 36:557–565. [PubMed: 7944288]
- Higuchi T, Fernandez EJ, Maudsley AA, Shimizu H, Weiner MW, Weinstein PR. Mapping of lactate and N-acetyl-l-aspartate predicts infarction during acute focal ischemia: in vivo 1H magnetic resonance spectroscopy in rats. *Neurosurgery*. 1996; 38:121–129. discussion 129–130. [PubMed: 8747960]
- Monsein LH, Mathews VP, Barker PB, Pardo CA, Blackband SJ, Whitlow WD, et al. Irreversible regional cerebral ischemia: serial MR imaging and proton MR spectroscopy in a nonhuman primate model. *AJNR Am J Neuroradiol*. 1993; 14:963–970. [PubMed: 8352171]
- Guadagno JV, Warburton EA, Jones PS, Day DJ, Aigbirhio FI, Fryer TD, et al. How affected is oxygen metabolism in DWI lesions? A combined acute stroke PET-MR study. *Neurology*. 2006; 67:824. [PubMed: 16966545]

15. Parsons MW. Acute hyperglycemia adversely affects stroke outcome: a magnetic resonance imaging and spectroscopy study. *Ann Neurol.* 2002; 52:20–28. [PubMed: 12112043]
16. Capes SE, Hunt D, Malmberg K, Pathak P, Gerstein HC. Stress hyper-glycemia and prognosis of stroke in nondiabetic and diabetic patients—a systematic overview. *Stroke.* 2001; 32:2426–2432. [PubMed: 11588337]



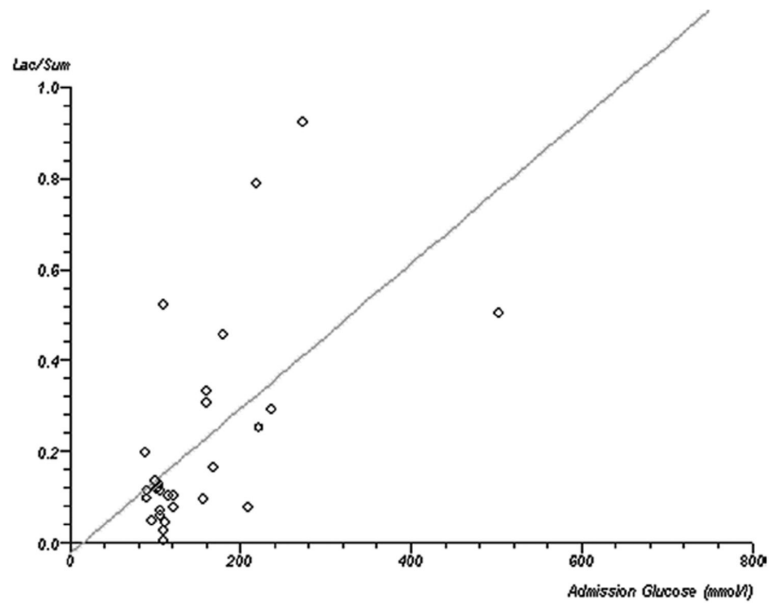


**Figure 1.** Correlation between serum glucose concentration and brain lactate. Scatterplot with regression line demonstrating the correlation between baseline glucose concentration (x-axis, mmol/L) and brain tissue lactate concentration on subject-wise data.

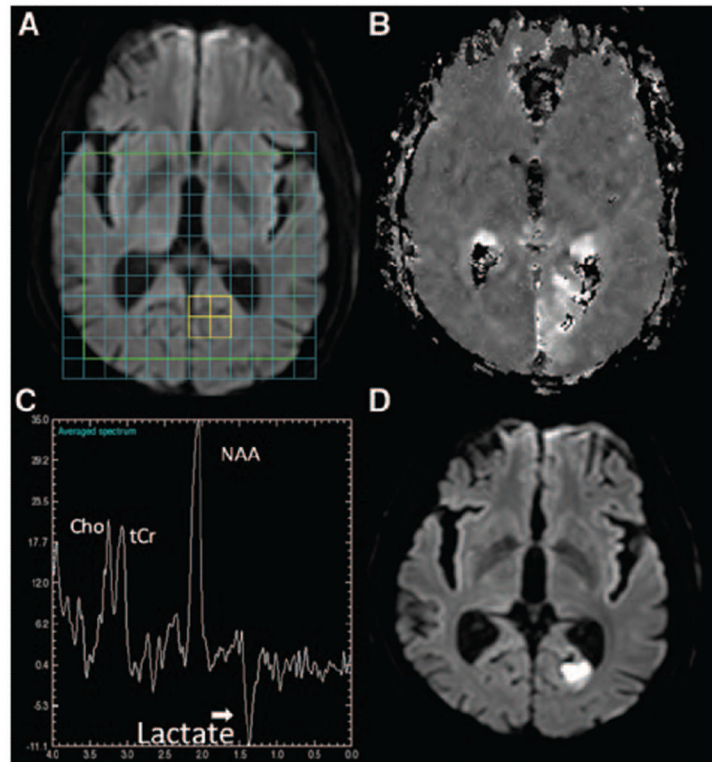


**Figure 2.**

Lactate in a region of total PWI–DWI mismatch. **A**, Baseline DWI with overlaid spectroscopy grid. The colored voxels in the left occipital lobe highlight the region corresponding to the spectrum in **C**. **B**, Baseline unthresholded map of MTT. **C**, The metabolite spectrum. The x-axis is in units of parts per million (ppm) and the y-axis is in arbitrary units. **D**, Follow up DWI at 24 hours shows a lesion in the left occipital lobe. A Lac peak is seen at 1.33 ppm with NAA (2.01 ppm), Cho (3.22 ppm) and tCr (3.03 ppm) peaks also visible. PWI indicates perfusion-weighted imaging; DWI, diffusion-weighted imaging; MTT, mean transit time; Lac, lactate; NAA, N-acetyl-L-aspartate; Cho, choline; tCr, total creatine.

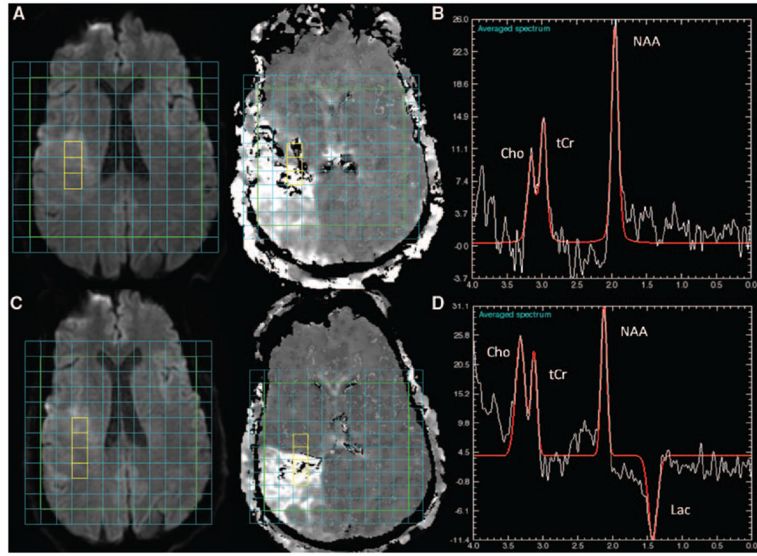


**Figure 3.** Delayed detection of lactate in the DWI lesion images from Subject 14, imaged at 2.2 hours (A–B) and 2 hours later (C–D). Although there is a lesion on baseline DWI (A, left) and a delayed MTT (A, right), there was no Lac detected at 2.2 hours (B). Associated with the stroke seen on follow DWI (C, left) and MTT (C, right), Lac was clearly detectable at 1.33 ppm (D) at follow-up. NAA, Cho, and tCr peaks are seen on both spectra (C, and F). DWI indicates diffusion-weighted imaging; MTT, mean transit time; Lac, lactate; NAA, N-acetyl-l-aspartate; Cho, choline; tCr, total creatine.

Table

Basic Clinical and Spectroscopic Data for Each Included Subject\*

Subject No.	Time Since Last Seen Normal, h	Age, y	Sex	Admission NIHSS	Admission Glucose, mg/dL	DWI Lesion Volume, mL	No. of Voxels Analyzed	Lac/Sum	NAA/Sum	Cho/Sum	Cr/Sum
1	1.3	58	Female	4	208	3	1	0.08	0.44	0.32	0.24
2	18.3	80	Male	11	273	88	2	0.92	0.69	0.54	0.54
3	4.4	71	Female	26	91	98	2	0.10	0.52	0.24	0.33
4	19.0	57	Female	26	236	39	9	0.29	0.33	0.23	0.21
5	2.9	72	Male	40	180	127	6	0.46	0.25	0.29	0.25
6	11.4	54	Male	8	503	23	4	0.51	0.40	0.35	0.35
7	5.8	91	Male	5	109	5	2	0.52	0.48	0.71	0.69
8	3.6	74	Male	9	90	83	7	0.11	0.50	0.26	0.35
9	4.9	60	Male	5	161	8	1	0.31	0.17	0.14	0.23
10	23.7	81	Female	4	95	1	1	0.05	0.46	0.18	0.58
11	4.7	54	Male	20	101	122	9	0.12	0.37	0.22	0.26
12	8.3	65	Male	14	156	106	5	0.09	0.07	0.04	0.05
13	3.7	53	Male	6	109	1	1	0.03	0.69	0.32	0.34
14	2.2	71	Male	5	110	22	8	0.01	0.49	0.22	0.28
15	4.9	65	Female	5	161	14	2	0.33	0.36	0.25	0.29
16	1.6	45	Male	3	104	1	1	0.12	0.54	0.34	0.34
17	3.4	77	Female	14	116	52	5	0.10	0.10	0.10	0.10
18	2.8	53	Female	8	122	27	3	0.11	0.29	0.28	0.35
19	4.4	85	Male	26	219	291	12	0.79	0.87	0.82	0.66
20	7.2	82	Female	13	100	9	5	0.14	0.57	0.16	0.24
21	3.4	48	Female	2	106	3	2	0.11	0.55	0.22	0.36
22	24.0	74	Female	7	111	5	8	0.05	0.45	0.28	0.25
23	7.4	53	Male	6	167	10	6	0.17	0.20	0.21	0.21
24	1.7	70	Male	4	115	0	2	†	†	†	†
25	22.8	86	Male	19	103	12	2	0.13	0.34	0.19	0.29
26	6.9	78	Female	4	84	2	3	†	†	†	†
27	2.7	77	Male	17	112	30	3	†	†	†	†
28	5.7	44	Male	40	106	13	7	0.07	0.36	0.23	0.31

Subject No.	Time Since Last Seen Normal, h	Age, y	Sex	Admission NIHSS	Admission Glucose, mg/dL	DWI Lesion Volume, mL	No. of Voxels Analyzed	Lac/Sum	NAA/Sum	Cho/Sum	Cr/Sum
29	2.0	61	Female	12	89	77	7	0.20	0.34	0.40	0.27
30	2.7	53	Female	16	221	23	5	0.25	0.33	0.30	0.25
31	2.6	53	Female	16	105	12	2	0.06	0.28	0.32	0.20
32	17.9	78	Male	25	122	92	3	0.08	0.22	0.22	0.24

NIHSS indicates National Institutes of Health Stroke Scale; DWI, diffusion-weighted imaging; Lac, lactate; NAA, N-acetylaspartate; Cho, choline; Cr, creatine.

\* Data for metabolite/sum are for voxels from the DWI lesion of each subject.

<sup>†</sup> Data unavailable.